

Air gap influence on the vibro-acoustic response of Solar Arrays during launch

J. López Díez (1), M. Chimeno Manguán (1), F. Simón Hidalgo (2),
J. Santiago Prowald (3), J.J. Wijker (4), J. García Echebarria (1) and M.J. Fernández (2)

(1) ETSI Aeronáuticos, Universidad Politécnica de Madrid (UPM), Madrid, Spain
(2) Instituto de acústica, Consejo Superior de Investigaciones científicas-UPM, Madrid, Spain
(3) European Space Agency, Noordwijk, The Netherlands
(4) Dutch Space B.V., Leiden, The Netherlands

PACS: 43.40 At

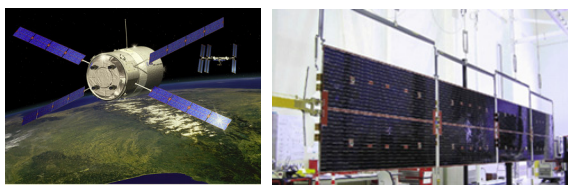
ABSTRACT

One of the primary elements on the space missions is the electrical power subsystem, for which the critical component is the solar array. The behaviour of these elements during the ascent phase of the launch is critical for avoiding damages on the solar panels, which are the primary source of energy for the satellite in its final configuration. The vibro-acoustic response to the sound pressure depends on the solar array size, mass, stiffness and gap thickness. The stowed configuration of the solar array consists of a multiple system composed of structural elements and the air layers between panels. The effect of the air between panels on the behaviour of the system affects the frequency response of the system not only modifying the natural frequencies of the wings but also as interaction path between the wings of the array. The usual methods to analyze the vibro-acoustic response of structures are the FE and BE methods for the low frequency range and the SEA formulation for the high frequency range. The main issue in the latter method is, on one hand, selecting the appropriate subsystems, and, on the other, identifying the parameters of the energetic system: the internal and coupling loss factors. From the experimental point of view, the subsystems parameters can be identified by exciting each subsystem and measuring the energy of all the subsystems composing the Solar Array. Although theoretically possible, in practice it is difficult to apply loads on the air gaps. To analyse this situation, two different approaches can be studied depending on whether the air gaps between the panels are included explicitly in the problem or not. For a particular case of a solar array of three wings in stowed configuration both modelling philosophies are compared. This stowed configuration of a three wing solar arrays in stowed configuration has been tested in an acoustic chamber. The measured data on the solar wings allows, in general, determining the loss factors of the configuration. The paper presents a test description and measurements on the structure, in terms of the acceleration power spectral density. Finally, the performance of each modelling technique has been evaluated by comparison between simulations with experimental results on a spacecraft solar array and the influence on the apparent properties of the system in terms of the SEA loss factors has been analysed.

INTRODUCTION

This work is devoted to the analysis of the response of spacecraft structural components to random acoustic loads and to the correlation between analytical and testing results.

During the ascent phase of the launch, one of the main critical loads affecting the mission are the vibro-acoustic loads produced by the jet mixing, boundary layer and rocket engines generated noise. These loads affect structurally the solar arrays as main component of the power subsystem. Hence, the response of this element (system) to acoustic random load is one of the load cases to be studied both theoretically and experimentally.



(Source: Courtesy of ESA and Dutch Space, 2008)

Figure 1. Rendering of ATV and solar array in deployed configuration during ground test

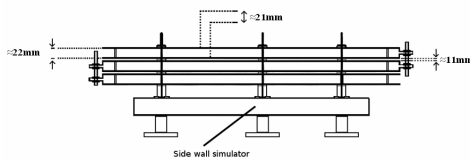
Figure 1 presents pictures of the ATV spacecraft and one of its solar arrays in deployed configuration. Figure 2 depicts one of the solar arrays during test in stowed configurations. In the last one, the relative thickness of the air gap between panels and panel thickness is shown in the zoomed region.

Numerical analyses are usually developed using two different model philosophies: FEM/BEM (Finite element models for the structural components, the panels, and air confined in the gaps between panels; the boundary element method, if unbounded air surrounds the system), and SEA (Statistical Energy Analysis) to study the response in the high frequency range (high modal density). This paper is focused on this last methodology.

SEA [1 to 3] evaluates the system behaviour in terms of power flow between the different subsystems. The main parameters used to characterize the energetic subsystems that constitute the problem are the SEA loss factors: the internal loss factors (ILF), which represent the dissipation of energy in each subsystem, and the coupling loss factors (CLF) that represent the power flow through subsystems; additionally the modal density of each component completes the system definition.

Knowing these parameters allows analysing the power balance formulated by SEA, which compares the power input to each subsystem with the energy stored and exchanged between subsystems. Once models are developed, the spacecraft component is usually tested to experimentally verify the model data. For this task, the most common methodology is the Power Injection Method (PIM) [4, 5] that considers the successive injection of power on the subsystems that make up the system. Through PIM, by successively applying power to each subsystem and measuring the energy stored in all the subsystems, a set of power balance equations allows obtaining the loss factors matrix characterizing the structure. On this aspect, literature presents different algorithms and experimental techniques to improve the results or determine the modal density of each component.

From the experimental point of view, to apply loads on and to measure the response of every single subsystem can be sometimes a hard task. One of these cases is the analysis of large solar arrays in stowed configuration, which is the leitmotiv of this work. Figure 2 sketches typical dimensions of these components. A typical length to width ratio of the wings of the solar array is 1.2 being 2.5 m a typical length for the shorter side. The typical thickness of the panel is 22 mm while the gap thickness between the wings is of the order of 11 mm. These typical dimensions agree with the ones corresponding to the ARA-MK3 (Dutch Space) solar array that will be studied within this work. The system is composed by three solar panels as depicted in Figure 2. Each panel is instrumented with accelerometers, as in Figure 3. Pressure sensors could be placed between panels to measure the pressure on the cavities, but due to its thickness special sensors are required.



(Source: Courtesy of Dutch Space, 2009)

Figure 2. On top, sketch of the stowed configuration of the ARA-MK3 solar array in stowed configuration. On bottom, the solar array during acoustic tests. Detail shows the gap thickness between panels

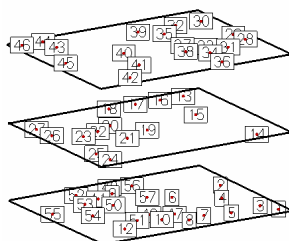


Figure 3. Accelerometers distribution on the three array wings for measuring the response of the ARA-MK3 during the Power Injection Method test

The influence of these air layers and the fluid-structure interaction drastically affects the structural response of the system [6 to 8], but exciting and measuring on all the subsystems (air gaps and middle panel) is far from obvious.

The particularities of a solar array in stowed configurations, as inaccessibility to the middle wing, affect the applicability of the PIM in the traditional procedure. Applicability of the PIM regarding the influence of the numerical issues associated to experimental results, and alternative expressions of the power balance as the Experimental SEA (ESEA) have been proposed [9].

This paper analyses different techniques to study the effect of the subsystem coupling on the loss factors matrix. The second section presents the theoretical aspects of the proposed method. It first shows the effective loss factor matrix governing the measured and excited subsystems when only a subset of the SEA subsystems can be excited and measured, showing that the resulting matrix is not enough to satisfy the traditional relationships [4]. Additionally, as is shown in Figure 2, some subsystems response can be measured but injecting loads into them can be difficult, as is the case of the middle plate. In testing specimens, holes can be drilled in the external panels in order to access and excite the medium panel, [10], but this is not the case with flight models. Given these conditions, an optimization process is proposed to determine the optimal reduced loss factors matrix by satisfying the equation and minimizing the variation of the coefficients with respect to the model. Finally, a similar procedure is proposed, studying the original model without reducing its subsystems definition to the experimental measured subsystems.

The third section simulates a system of three circular plates with two air layers, and applies the proposed procedure to show its viability and the influence of the selection of the considered subsystems. Finally, the fourth section describes the test carried out on the Figure 2 specimen, and applies the different procedures in order to estimate the loss factors matrix through the canonical application of the PIM and also taking into account the considerations presented in this work.

THEORETICAL MODEL

Basic Formulation

SEA is a stochastic methodology that analyses the power balance of a system in terms of the power input to the system, the power dissipated in the system and the power flow between the different elements or subsystems that make it up, that are analysed through their energy dissipation (internally or as power transferred to other subsystems). SEA analyses the power balance of an ensemble of specimens of the problem studied in terms of the frequency averaged magnitudes of the system (energy or power input).

Within a set of g subsystems, for a certain subsystem i , the power balance can be expressed in terms of the input power applied to the subsystem (P_i), the internally dissipated energy (through the internal loss factor η_{ii}) and the power transferred between the analysed subsystems and the other ones (through the coupling loss factors η_{ij} and η_{ji}), both expressed as function of the energy of the subsystem E_j :

$$P_i = \omega E_i \sum_{j=1}^g \eta_{ij} - \omega \sum_{\substack{j=1 \\ j \neq i}}^g E_j \eta_{ji} \quad (1)$$

The global power balance for the whole system under a certain input power state on the several subsystems is characterized, for each frequency band centred in ω studied, by the SEA matrix relationship:

$$\{P\} = \omega [L] \{E\} \quad (2)$$

Where $\{P\}$ stands for the power applied to each subsystem at each frequency band and the vector $\{E\}$ contains the energy of each subsystem. Both of them are vectors of g elements. Finally, the loss factors matrix, $[L]$, is $g \times g$ matrix, with negative values for the terms out of the main diagonal, and positive values on the diagonal. Writing equation 2 in expanded format:

$$\begin{Bmatrix} P_1 \\ \vdots \\ P_i \\ \vdots \\ P_g \end{Bmatrix} = \omega \begin{bmatrix} \sum_{j=1}^g \eta_{1j} & \cdots & -\eta_{1i} & \cdots & -\eta_{1g} \\ \vdots & \ddots & \vdots & \ddots & \vdots \\ -\eta_{i1} & & \sum_{j=1}^g \eta_{ij} & & -\eta_{ig} \\ \vdots & & \vdots & \ddots & \vdots \\ -\eta_{1g} & \cdots & -\eta_{ig} & \cdots & \sum_{j=1}^g \eta_{gj} \end{bmatrix} \begin{Bmatrix} E_1 \\ \vdots \\ E_i \\ \vdots \\ E_g \end{Bmatrix} \quad (3)$$

The PIM [4] is based on studying of the system under successive input power to the g subsystems to obtain g equations of the form of Eq.(2). The resulting set of g^2 equations that allows obtaining the SEA loss factors can be rearranged considering the power as the independent terms and the SEA loss factors as variables, instead of the energies,

$$\begin{Bmatrix} P_1 \\ 0 \\ 0 \\ 0 \\ 0 \\ 0 \\ 0 \\ 0 \\ 0 \\ 0 \end{Bmatrix} = \omega \begin{bmatrix} E_1^1 & E_1^1 & E_1^1 & -E_1^1 & 0 & 0 & -E_g^1 & 0 & 0 \\ 0 & -E_1^1 & 0 & E_1^1 & E_1^1 & E_1^1 & 0 & -E_g^1 & 0 \\ 0 & 0 & -E_1^1 & 0 & 0 & -E_1^1 & E_g^1 & E_g^1 & E_g^1 \\ \vdots & \vdots \\ 0 & E_1^i & E_1^i & E_1^i & -E_1^i & 0 & 0 & -E_g^i & 0 \\ 0 & 0 & -E_1^i & 0 & E_1^i & E_1^i & E_1^i & 0 & -E_g^i \\ 0 & 0 & -E_1^i & 0 & 0 & -E_1^i & E_g^i & E_g^i & E_g^i \\ \vdots & \vdots \\ 0 & E_1^g & E_1^g & E_1^g & -E_1^g & 0 & 0 & -E_g^g & 0 \\ 0 & 0 & -E_1^g & 0 & E_1^g & E_1^g & E_1^g & 0 & -E_g^g \\ 0 & 0 & -E_1^g & 0 & 0 & -E_1^g & E_g^g & E_g^g & E_g^g \end{bmatrix} \begin{Bmatrix} \eta_{11} \\ \eta_{1i} \\ \eta_{1g} \\ \eta_{ii} \\ \eta_{ig} \\ \eta_{gg} \\ \eta_{g1} \\ \eta_{gi} \\ \eta_{gg} \end{Bmatrix} \quad (4)$$

The energies of the subsystems under the several input power conform the energy matrix displayed where E_i^j denotes the energy of the subsystem i when the subsystem j is excited.

The canonical formulation of the PIM implies the injection of power on all the g subsystems that are considered on the system to obtain the g^2 loss factors. It also requires measuring the response on the g subsystems to determine the energy matrix on equation 4. As stated before, these two requirements may not be fulfilled due to the particularities of the configurations to study.

The influence of these restrictions on the knowledge of the system response is presented. For the case in which it is not possible to determine the whole response of the system (named as internal knowledge) because it is not possible to measure on all the subsystems considered, an effective loss matrix that governs the apparent response of the system will be presented. For the case in which it is not possible to determine enough power balance states under external loads for the system (named as external knowledge) a procedure to derive the loss factors from a set of reduced cases will be presented.

Reduced Model

In general, for PIM applications each subsystem is excited and the applied power as well as the energy in each subsystem is measured.

For the case of studying a complete satellite, or the solar array in Figure 2, it is not possible to apply power on all the subsystems. In particular, to excite the subsystem corresponding to the gaps is not a standard activity during test campaign [10].

In this case, a reduction philosophy, [11, 12], can be applied and the subsystems can be classified as those in which power is applied and energy is measured, and the remaining ones. The first kind of subsystems is the so-called 'analysed' and the other 'omitted'.

Equation 3 can be divided into two sets of equations, as in the static reduction for FE models [11] formulating together the whole system, distinguishing between subsystem in which loads are applied, designed with subscript e for excited, and those in which no power is applied, designed as o for omitted:

$$\begin{Bmatrix} [P_e] \\ [0] \end{Bmatrix} = \omega \begin{bmatrix} [L_{ee}] & [L_{eo}] \\ [L_{oe}] & [L_{oo}] \end{bmatrix} \begin{Bmatrix} [E_e] \\ [E_o] \end{Bmatrix} \quad (5)$$

Where:

$[P_e]$ is a square matrix of e rows and columns containing the power applied to the subsystems which are excited successively, and their energy measured; usually a diagonal matrix.

$[0]$ is a zero matrix of $g-e$ rows and e columns.

$[E_e]$ is a square matrix of e rows and columns containing the energy measured on the subsystem in which power is applied.

$[E_o]$ is a matrix of $g-e$ rows and e columns containing the energy of the subsystems in which either the energy is not measured or power is not applied.

$[L_{oo}]$ is the partition of the matrix corresponding to the set of omitted subsystems of $g-e$ rows and $g-e$ columns

$[L_{oe}]$ is the partition of the matrix corresponding to the coupling of subsystems having $g-e$ rows and e columns.

$[L_{eo}]$ is the partition of the matrix corresponding to the coupling of subsystems having e rows and $g-e$ columns.

The lower set of equations in equation 5 relates the energies of the omitted and analysis subsystems.

$$[0] = \omega \left([L_{oe}] [E_e] + [L_{oo}] [E_o] \right) \quad (6)$$

Then, the energy level on the omitted subsystems can be determined from the energy measured on the excited subsystems, as in the static reduction, [11]:

$$[E_o] = -[L_{oo}]^{-1} [L_{oe}] [E_e] \quad (7)$$

Finally, the relationship between the power applied and the energy on the excited subsystems results:

$$\begin{aligned}
[P_e] &= \omega \left([L_{ee}] [E_e] + [L_{eo}] [E_o] \right) = \\
&= \omega \left([L_{ee}] - [L_{eo}] [L_{oo}]^{-1} [L_{oe}] \right) [E_e] \quad (8) \\
&= \omega [LR_{ee}] [E_e]
\end{aligned}$$

Being:

$$[LR_{ee}] = [L_{ee}] - [L_{eo}] [L_{oo}]^{-1} [L_{oe}] \quad (9)$$

the reduced or effective loss matrix (ELM).

This formulation points out the influence of the selection of the subsystems for the final result of the loss matrix. For a set of subsystems, the PIM allows to calculate directly only the reduced or effective loss matrix $[LR_{ee}]$

As a conclusion, when the excited and the measured subsystems are not the complete set of subsystems, the experimentally determined loss matrix is not the one engaged with the complete system. Additionally, the coefficients of the reduced matrix are not obliged to fulfil the requirements of the complete system.

Determination of the effective SEA loss matrix

Commonly, the number of subsystems in which the energy can be measured is greater than the ones in which load is applied. In this case, the number of equation is not enough to apply directly the PIM neither for the original set of subsystems nor for the reduced set analysed in the previous paragraph. To estimate the damping loss matrix a procedure based on updating techniques is proposed.

In general, m subsystems could be measured, while only e subsystems are excited. In this case, equation 3 converts to:

$$\begin{bmatrix} [P_m] \\ [0] \end{bmatrix} = \omega \begin{bmatrix} [L_{mm}] & [L_{mo}] \\ [L_{om}] & [L_{oo}] \end{bmatrix} \begin{bmatrix} [E_m] \\ [E_o] \end{bmatrix} \quad (10)$$

Where:

$[P_m]$ is a rectangular matrix of m rows and e columns.

$[0]$ is a zero matrix of $g-m$ rows and e columns.

$[E_m]$ is a matrix of m rows and e columns containing the energy measured on the subsystem in which power is applied.

$[E_o]$ is a matrix of $g-m$ rows and e columns containing the energy of the subsystems in which either the energy is not measured or power is not applied.

$[L_{oo}]$ is the partition of the matrix corresponding to the set of omitted subsystems.

$[L_{om}]$ is the partition of the matrix corresponding to the coupling of subsystem having $g-m$ rows and m columns.

$[L_{mo}]$ is the partition of the matrix corresponding to the coupling of subsystem having m rows and $g-m$ columns.

In this case, the system can be reduced as:

$$\begin{aligned}
[P_m] &= \omega \left([L_{mm}] [E_m] + [L_{mo}] [E_o] \right) = \\
&= \omega \left([L_{mm}] - [L_{mo}] [L_{oo}]^{-1} [L_{om}] \right) [E_m] \quad (11) \\
&= \omega [LR_{mm}] [E_m]
\end{aligned}$$

This theoretical expression can also be interpreted when experimental measurements are available. In general, it is not possible to apply loads experimentally on all subsystems, and then, the determination of the effective power loss matrix cannot be estimated directly by application of the PIM, as in the previous case. The proposed formulation takes into account the lower level of information due to not having as many load cases as subsystems considered, obtaining the loss factors matrix from less information than in previous subsection.

The proposed methodology is based on correcting the matrix of the model to update it based on the experimentally measured powers and energies.

The purpose here is to calculate the Effective Loss Matrix of the reduced system, $[LR_{mm}]$, that approximates the most to the Analytical Effective Loss Matrix, $[LR_{mm}^A]$, obtained by reducing the analytical loss factor matrix.

The update of the dissipation matrix is performed imposing the condition of fulfilling the measured power balance and minimizing the following functional that impose the closure between the analytical and the updated matrix, [13 and 14]:

$$J = \frac{1}{2} \left\| [N] \left([LR^A] - [LR] \right) [N] \right\| \quad (12)$$

Where $[N]$ is a normalization matrix that is chosen as $N = [LR_{mm}^A]^{-1/2}$

The additional constraint related with the measured cases is:

$$[P_m] - \omega [LR_{mm}] [E_m] = 0 \quad (13)$$

To impose the additional condition of fulfilling the measured energetic states, equation 13 is included in the functional through a set of Lagrange's multipliers in the form:

$$\begin{aligned}
J &= \frac{1}{2} \sum_{i,j=1}^m \sum_{h,k=1}^m \left[[N]_{ih} \left([LR^A]_{hk} - [LR]_{hk} \right) [N]_{kj} \right]^2 + \\
&+ \sum_{h=1}^m \sum_{j=1}^e \lambda_{hj} \left[[P]_{hj} - \omega \sum_{k=1}^m [LR]_{hk} [E]_{kj} \right] \quad (14)
\end{aligned}$$

The augmented function is now minimized with respect to the $m \times m$ elements of the corrected dissipation matrix $[LR]_{hk}$ obtaining the condition of minimization of the functional, J :

$$[N]^2 \left([LR^A] - [LR] \right) [N]^2 - \omega [\lambda] [E]^T = 0 \quad (15)$$

Incorporation of the additional conditions in (13) allows obtaining an expression for the Lagrange's multipliers that allow rewriting the updating law as:

$$[LR] = [LR^A] + \frac{1}{\omega} [\Delta P_m] [IE_m] \quad (16)$$

With

$$[\Delta P_m] = [P_m] - \omega [LR^A] [E_m] \quad (17)$$

and

$$[IE_m] = \left([E_m]^T [N]^{-2} [E_m] \right)^{-1} [E_m]^T [N]^{-2} \quad (18)$$

The presented updating law allows calculating the effective SEA loss factors matrix of the system (that will be the theoretical one if the whole system is considered) taking into account the power balance states measured in both cases of full or partial external knowledge (if the number of cases available is equal to the number of subsystems considered or not). A summary of the considerations to evaluate in order to apply the updating technique presented are summarized in Table 1 in function of the size of the system considered (whole or reduced) and the number of input power cases (external knowledge).

Table 1. Summary of updating procedure depending on number of input power cases known, being $[P]$ and $[E]$ the corresponding input power and energy of the subsystems; $[L^A]$ the loss matrix of the model and $[L]$ the sea loss matrix determined (effective in the case of the reduced system)

	Whole system (g subsystems) (g ² variables)		Reduced system (m subsystems) (m ² variables)	
	Full e = g	Reduced e ≠ g	Full e = m	Reduced e ≠ m
Level of External Knowledge (set of cases)				
Model Dissipation Matrix	$[L^A]$ g x g		$[L^A]$ m x m	
Constraints $[P] = \omega[L][E]$	$\begin{matrix} [P] & [L] & [E] \\ g \times g & g \times g & g \times g \end{matrix}$	$\begin{matrix} [P] & [L] & [E] \\ g \times g & g \times g & g \times g \end{matrix}$	$\begin{matrix} [P] & [L] & [E] \\ m \times m & m \times m & m \times m \end{matrix}$	$\begin{matrix} [P] & [L] & [E] \\ m \times m & m \times m & m \times m \end{matrix}$

Partial Internal Knowledge

Considering a system made up of s subsystems, in which only a reduced set of r subsystems can be evaluated, the dissipation matrix of the system, the full matrix, engages s² SEA loss factors, while the additional constraints due to the known energetic states are expressed in terms of the effective dissipation matrix that is made up of the r² effective SEA loss factors. This is the case of the folded configuration of solar array in which to excite the middle panel may not be feasible [10]. In this case, it is necessary to obtain the effective dissipation matrix due to the reduction of the system from the whole system to the measurable set of subsystems. A summary of the considerations to evaluate in order to apply the updating technique presented are summarized in Table 2 for a given size of the system in function of the size of the system that can be measured (internal knowledge) and the number of input power cases (external knowledge).

Table 2. Summary of updating procedure when measured subsystems are less than those of interest depending on number of input power cases known, being $[P]$ and $[E]$ the corresponding input power and energy of the subsystems; $[L^A]$ the loss matrix of the model and $[L]$ the effective loss matrix determined

	g subsystems analysed (g ² variables)	
	m subsystems measured	
Level of Internal Knowledge		
Level of External Knowledge	Full e = m states known	Reduced e ≠ m states known
Model Dissipation Matrix	$[L^A]$ g x g	
Constraints $[P] = \omega[L][E]$	$\begin{matrix} [P] & [L] & [E] \\ m \times m & m \times m & m \times m \end{matrix}$	$\begin{matrix} [P] & [L] & [E] \\ m \times m & m \times m & m \times m \end{matrix}$

SIMULATED MODEL

This section presents the application of the previous theoretical considerations to an analytical model representing the kind of behaviour appearing in the folded configuration of solar arrays. The system, depicted in Figure 4, is made of three circular plates (of 0.3 m of diameter and a thickness of 0.001 m) close together at a distance of 0.012 m. The two corresponding air layers between the plates (with standard air properties, c = 343 m/s and a density of 1.21 kg/m³) are considered. The different plates are only coupled through the air layers, without a direct connection between them. The two air layers are coupled through the middle plate, with no direct connection between them. No external air is considered in the model. The dissipation loss factors of the system can be obtained directly for the configuration described and are taken as reference values for evaluating the methodologies presented.

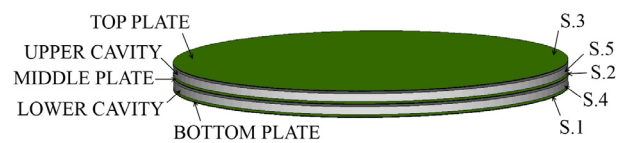


Figure 4. Sketch of the simulated model: System is compound of three circular plates connected only through air. Nomenclature for the plates, air layers, and subsystems is stated

The properties of the model suppose a modal density of the elements engaged high enough for the applicability of SEA.

To simulate a test based on the Power Injection Method, the system response is simulated in standard third octave bands from 16 Hz to 8000 Hz. Each element of the system (the three plates and the two air layers) are excited successively with a known input power of 1 W in each band and the response of the system to the applied load is computed obtaining the energy of each element of the system.

To evaluate the SEA loss factors of the case proposed, the previous procedures are applied under three levels of analysis in function of the systems excited and measured:

- Excitation and measurement are allowed in the three plates that are also the three subsystems considered in the system (full internal and external knowledge), evaluating the effective dissipation matrix.
- While measurement in the three plates is considered, only excitation on the external panels is considered providing only two energetic states of the system (full internal knowledge, partial external knowledge), evaluating the effective dissipation matrix.
- Inclusion of the air layers as explicit subsystems is considered, expanding the system to a five subsystems problem, while only measurement in the three plates is considered and under excitation on the external plates only (partial internal and external knowledge), evaluating the whole dissipation matrix.

The power balance of the system presented is driven by the power inputs and the SEA loss factors corresponding to the internal and coupling power transfers. Given the identical properties of the plates and air layers only three loss factors

will be engaged: η_s and η_f the internal dissipation factors of the plates and air layers respectively; and η_{sf} and η_{fs} the coupling loss factor associated to the transfer of energy from the plate to the air layer and vice versa.

The following five subsystems are considered: Subsystem 1: Bottom Plate; Subsystem 2: Middle Plate; Subsystem 3: Top Plate; Subsystem 4: Lower Air Layer and Subsystem 5: Upper Air Layer. The energy balance for the stated subsystems can be expressed as:

$$\begin{Bmatrix} P_1 \\ P_2 \\ P_3 \\ P_4 \\ P_5 \end{Bmatrix} = \omega \begin{bmatrix} \eta_b + \eta_{ef} & 0 & 0 & -\eta_{es} & 0 \\ 0 & \eta_b + 2\eta_{ef} & 0 & -\eta_{es} & -\eta_{es} \\ 0 & 0 & \eta_t + \eta_{ef} & 0 & -\eta_{es} \\ -\eta_{ef} & -\eta_{ef} & 0 & \eta_t + 2\eta_{es} & 0 \\ 0 & -\eta_{ef} & -\eta_{ef} & 0 & \eta_t + 2\eta_{es} \end{bmatrix} \begin{Bmatrix} E_1 \\ E_2 \\ E_3 \\ E_4 \\ E_5 \end{Bmatrix} \quad (19)$$

If only the three plates are considered, rearranging the equation in the analysed and omitted subsystems allows rewriting the reduced effective dissipation matrix that relates the input powers to the energy of the plates in the form:

$$\begin{Bmatrix} P_1 \\ P_2 \\ P_3 \end{Bmatrix} = \omega \begin{bmatrix} \eta_b + \eta_{ef} - \frac{\eta_{ef}\eta_{es}}{\eta_t + 2\eta_{ef}} & -\frac{\eta_{ef}\eta_{es}}{\eta_t + 2\eta_{ef}} & 0 \\ -\frac{\eta_{ef}\eta_{es}}{\eta_t + 2\eta_{ef}} & \eta_b + 2\eta_{ef} - \frac{2\eta_{ef}\eta_{es}}{\eta_t + 2\eta_{ef}} & -\frac{\eta_{ef}\eta_{es}}{\eta_t + 2\eta_{ef}} \\ 0 & -\frac{\eta_{ef}\eta_{es}}{\eta_t + 2\eta_{ef}} & \eta_t + \eta_{ef} - \frac{\eta_{ef}\eta_{es}}{\eta_t + 2\eta_{ef}} \end{bmatrix} \begin{Bmatrix} E_1 \\ E_2 \\ E_3 \end{Bmatrix} \quad (20)$$

The expression of the reduced effective dissipation matrix shows that the indirect coupling between the adjacent plates is incorporated through the air layer in the terms outside of the diagonal while the effective or apparent internal dissipation factors of the plates do include the radiation of energy to the air layers.

To study the behaviour of the procedures proposed an analysis of their sensitivity to the error on the model to be updated is presented. Given the full loss matrix of the model (Equation 19) different degrees of uncertainty on the model to be updated in terms of error on the proposed loss factors are considered:

- An initial error of 20% on the internal loss factors of the measured subsystems (elements at the diagonal of L_{mm} of Equation 10)
- An initial error of 20% on the coupling loss factors between the measured and non-measured subsystems (elements on L_{mo} and L_{om} on Equation 10)
- An initial error of 20% on the internal loss factors of the non-measured subsystems (elements at the diagonal of L_{oo} of Equation 10).

Figures 5 to 7 show the SEA loss factors determined for the updated model when the first level of analysis is considered (excitation and measurement on the three plates that are all the subsystems considered) The value of the updated loss factors are displayed together with the values of the reference values (the analytical loss factors of the reduced effective loss matrix).

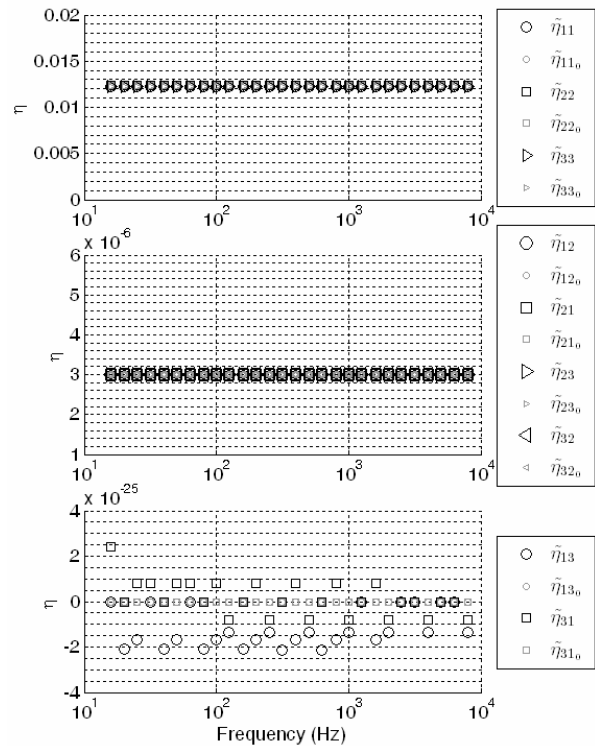


Figure 5. SEA loss factors of the reduced model (three plates) calculated through updating the model with a 20% of error on the ILF of the measured subsystems (black). Reference reduced values of the known solution in grey. From top to bottom internal dissipation factors; not null factors deduced from the reduced effective loss matrix and null factors as deduced from the reduced effective loss matrix

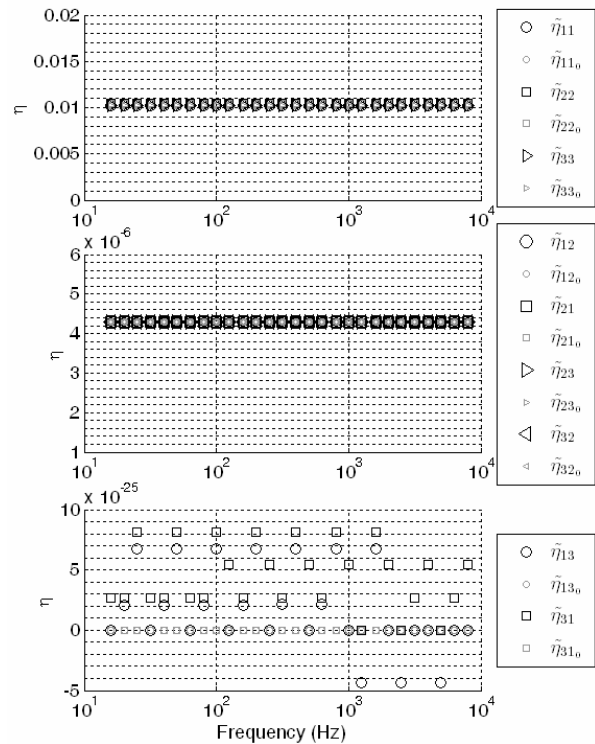


Figure 6. SEA loss factors of the reduced model (three plates) calculated through updating the model with a 20% of error on the CLF between measured and non-measured subsystems (black). Reference reduced values of the known solution in grey. From top to bottom internal dissipation factors; not null factors deduced from the reduced effective loss matrix and null factors as deduced from the reduced effective loss matrix

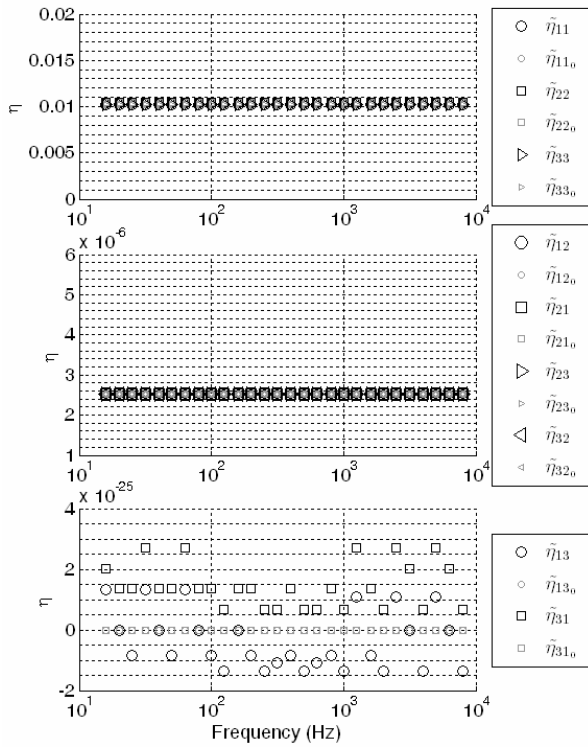


Figure 7. SEA loss factors of the reduced model (three plates) calculated through updating the model with a 20% of error on the ILF of the non-measured subsystems (black). Reference reduced values of the known solution in grey.

From top to bottom internal dissipation factors; not null factors deduced from the reduced effective loss matrix and null factors as deduced from the reduced effective loss matrix

From the results, it can be concluded that given full external knowledge on the system's response, exciting all the analysed subsystems, the updated model adequately predicts the response of the system even for the initial level of error considered, independently of the systems whose error it is associated to.

The results of the updating methodology to the second level of analysis that considers that excitation is allowed only on the external plates, imposing a lower level of knowledge on the systems response, are shown in Figures 8 to 13. Results, in terms of SEA loss factors and relative error (difference between the updated and actual value), are shown for the three degrees of uncertainty on the initial model.

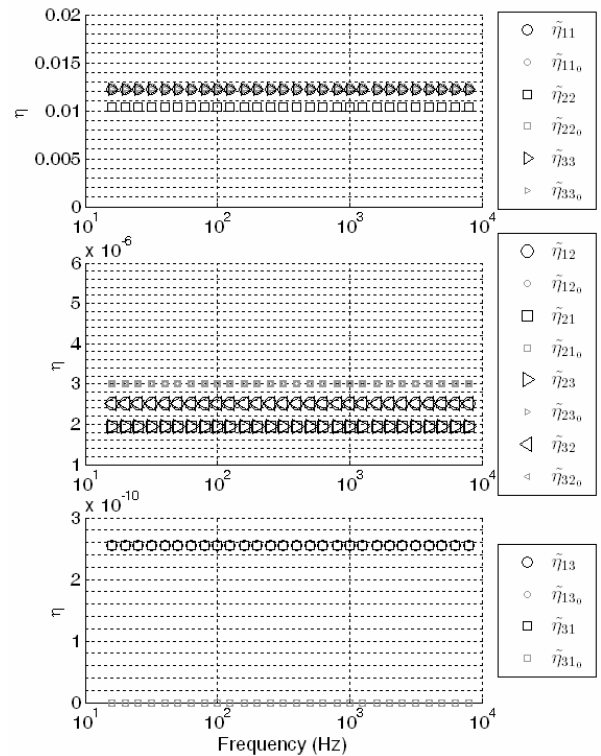


Figure 8. SEA loss factors of the reduced model (three plates), considering two power states exciting on the external plates only, updating the model with a 20% of error on the ILF of the measured subsystems (black). Reference reduced values of the known solution in grey. From top to bottom internal dissipation factors; not null factors deduced from the reduced effective loss matrix and null factors as deduced from the reduced effective loss matrix

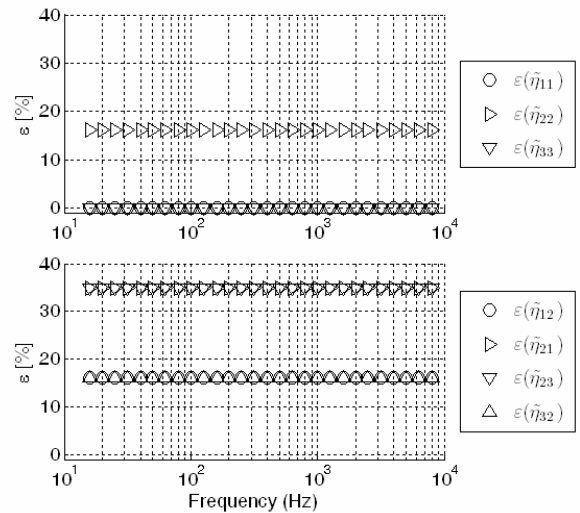


Figure 9. Relative error of the updated SEA loss factors of the reduced model (three plates), considering two power states exciting on the external plates only, updating the model with a 20% of error on the ILF of the measured subsystems (black). Values are shown for those factors which actual value is not null.

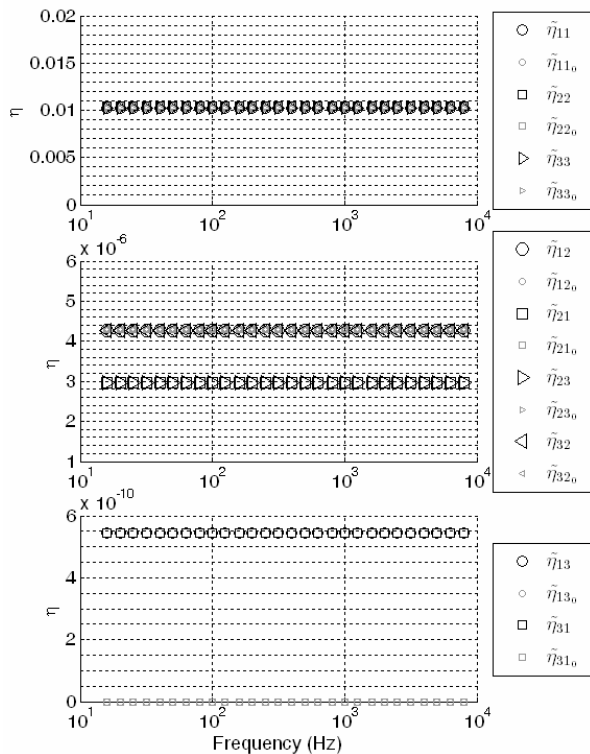


Figure 10. SEA loss factors of the reduced model (three plates), considering two power states exciting on the external plates only, updating the model with a 20% of error on the CLF between measured and non-measured subsystems (black). Reference reduced values of the known solution in grey. From top to bottom internal dissipation factors; not null factors deduced from the reduced effective loss matrix and null factors as deduced from the reduced effective loss matrix

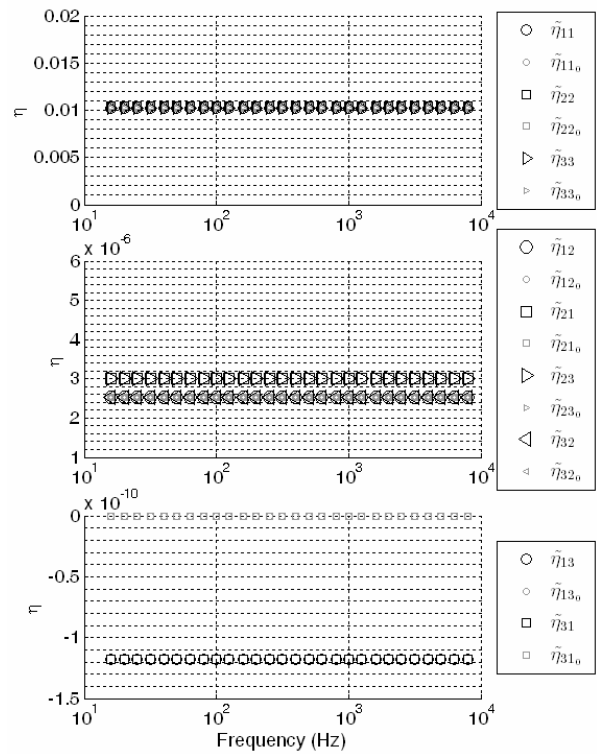


Figure 12. SEA loss factors of the reduced model (three plates), considering two power states exciting on the external plates only, updating the model with a 20% of error on the ILF of the non-measured subsystems (black). Reference reduced values of the known solution in grey. From top to bottom internal dissipation factors; not null factors deduced from the reduced effective loss matrix and null factors as deduced from the reduced effective loss matrix

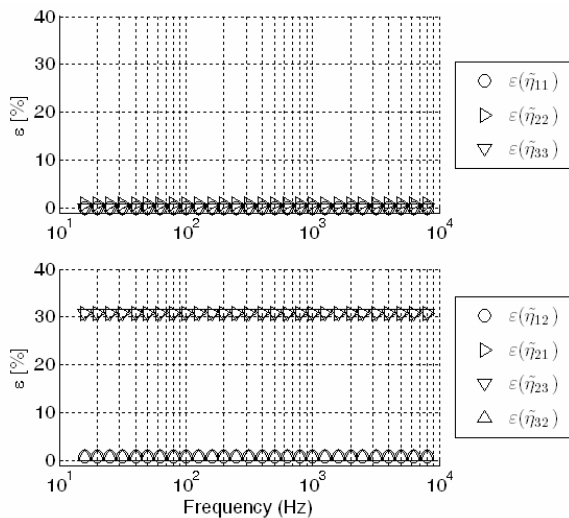


Figure 11. Relative error of the updated SEA loss factors of the reduced model (three plates), considering two power states exciting on the external plates only, updating the model with a 20% of error on the CLF between the measured and non-measured subsystems (black). Values are shown for those factors which actual value is not null.

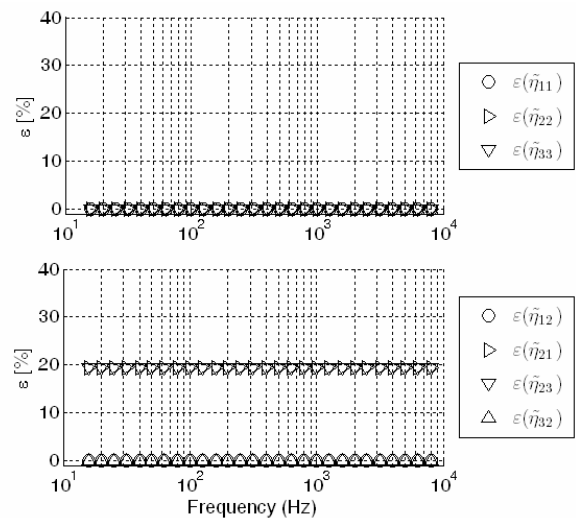


Figure 13. Relative error of the updated SEA loss factors of the reduced model (three plates), considering two power states exciting on the external plates only, updating the model with a 20% of error on the ILF of the non-measured subsystems (black). Values are shown for those factors which actual value is not null.

Two different behaviours can be concluded from previous figures for the internal and the coupling loss factors:

The accuracy of the ILF on the updated model is more affected by the uncertainty on the ILF of the measured subsystems than on the non-measured ones. In particular, the ILF of the non-excited subsystems is highly affected by the exclusion of the power state corresponding to injecting power on it.

The uncertainty on the CLF between measured and non-measured subsystems and on the ILF of the non-measured affects mainly to the updated coupling factors, being higher the influence corresponding to the uncertainty between the two kinds of subsystems (measured and non-measured).

Due to the lower external knowledge on the response of the system given that only two power states are considered, independently of the subsystems (measured or not) affected by the initial uncertainty, the accuracy of the coupling loss factors associated to the transfer of power from the excited subsystems to the non-excited ones is higher than the opposite, associated to the transfer of power from the non-excited subsystems to the excited ones.

The third level of analysis proposed is to include neither the excited nor measured subsystems in the model. For the present case, the air layers between the panels are included in the system and applying the updating technique, starting from an analytical model for the whole system (made of the five subsystems), the updated SEA loss factors are predicted considering the three levels of uncertainty stated: on the ILF of the measured subsystems, on the CLF of the measured subsystems and ILF of the non-measured subsystems. The full expanded model is updated taking into account only the information from the power states and energies measured on the reduced system (partial internal and external knowledge).

The relative error of the updated SEA loss factors of the expanded model are shown in Figures from 14 to 16. The values of the SEA loss factors of the full model (not reduced) are shown as reference.

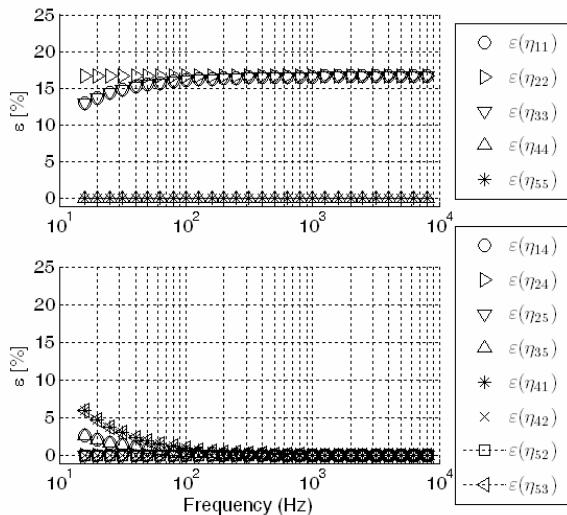


Figure 14. Relative error of the updated SEA loss factors of the expanded model (three plates and two air layers), considering two power states exciting on the external plates only, updating the model with a 20% of error on the ILF of the measured subsystems (black). Values are shown for those factors which actual value is not null.

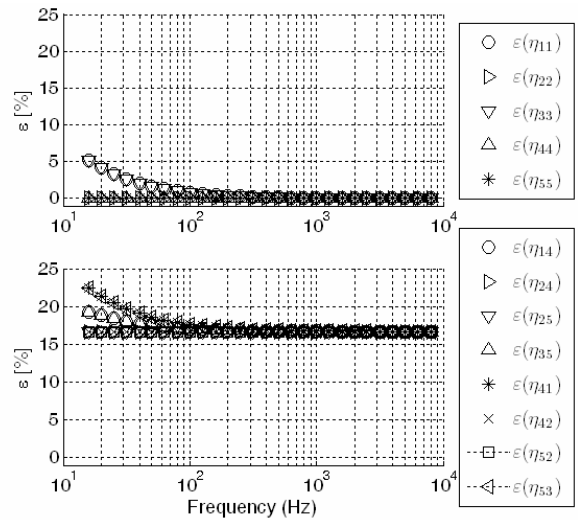


Figure 15. Relative error of the updated SEA loss factors of the expanded model (three plates and two air layers), considering two power states exciting on the external plates only, updating the model with a 20% of error on the CLF between the measured and non-measured subsystems (black). Values are shown for those factors which actual value is not null.

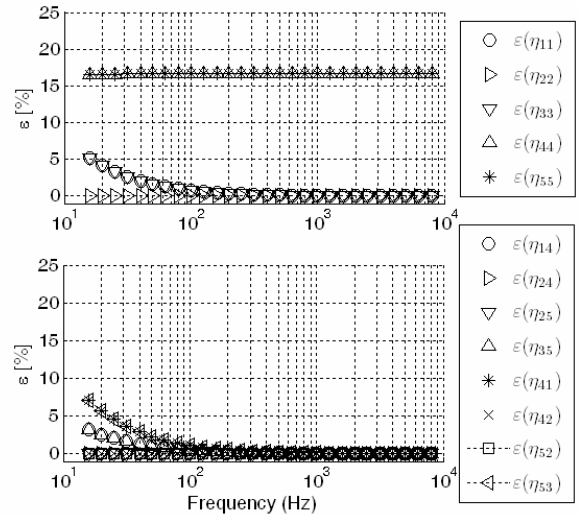


Figure 16. Relative error of the updated SEA loss factors of the expanded model (three plates and two air layers), considering two power states exciting on the external plates only, updating the model with a 20% of error on the ILF of the non-measured subsystems (black). Values are shown for those factors which actual value is not null.

Results show that a similar conclusion as for previous analyses can be stated. The uncertainty on the ILF of the starting model affects in a different degree depending on measuring or not the response of the system in which the uncertainty is considered. The main effect on the accuracy of the updated ILF is located in the uncertain systems

The uncertainty on the CLF between the measured and the non-measured subsystems affects mainly to the CLF of the updated model, slightly on a higher level on those corresponding to power transfer from the non-measured subsystems to measured subsystems.

A summary of the conclusions provided by the application of the three approaches proposed in function of the number of systems excited and measured is presented in table 3

Table 3. Summary of the application of the procedures presented applied to the analytical model.

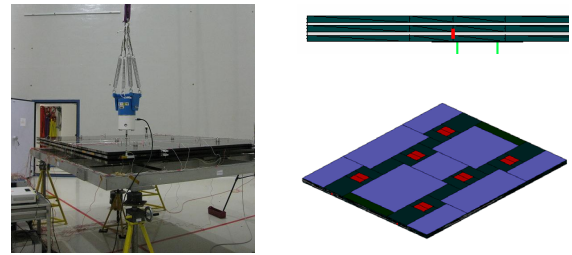
Method	Influence on results	
	Dependency on internal knowledge (reduced or full system)	Dependency on external knowledge (excitation of subsystems)
Inversion of Energy Matrix (Reduced system)	Greater apparent ILF due to radiation to omitted subsystems	Greater accuracy on CLF from excited to non-excited subsystems than reciprocal.
Updating Reduced Dissipation Matrix (Reduced system)	Greater apparent ILF due to radiation to omitted subsystems	Greater accuracy on CLF from excited to non-excited subsystems than reciprocal.
Updating Actual Dissipation Matrix (Full system)	Greater accuracy on CLF from excited to non-excited subsystems than reciprocal.	Greater accuracy on CLF from excited to non-excited subsystems than reciprocal.

This simple benchmark shows that to correctly identify the loss matrix using experimental data requires that the subsystems excited and measured will be similar to the original models. In the preset case, a methodology of reduction shows that, when excitation and measurements are not available for all the subsystems, the identification corresponds to a “reduced model”. The relationship between the original loss matrix and the identified experimentally, called effective loss matrix, has been formulated and verified numerically.

APPLICATION TO SEA LOSS FACTORS DETERMINATION OF SOLAR ARRAY

This paragraph presents the application of the previously stated methodologies to an actual specimen. The specimen studied is a breadboard model of a solar array of three panels, with a length to width ratio of 1.2, made on sandwich structure with aluminium core and CFRP skins with a total thickness of around 20 mm. The array wings are separated by a distance of around the half of the plate thickness conforming two air layer between the folded wings. The specimen instrumented for a Power Injection Method test is shown in Figure 17.

The particularities of the specimen, mainly the close distance between plates, drive the feasibility of a complete testing on the specimen: On one hand, considering the air layers as subsystems themselves would imply, in the classical approach for the Power Injection Method to not only measure the pressure field on the gap but also to excite the specimen applying power to the air layers. On the other hand, exciting the middle wing usually involves issues related to the accessibility to the inner area of the wing. Given these configuration related restrictions, the following subsystems are considered: Subsystem 1: Bottom Wing; Subsystem 2: Middle Wing; Subsystem 3: Top Wing; Subsystem 4: Lower Air Layer; Subsystem 5: Upper Air Layer. A model considering the stated subsystems oriented for predicting the response to acoustic load is depicted in Figure 17.



(Source: Courtesy of ESA and Dutch Space, 2009)

Figure 17. Three wings solar array in stowed configuration during a Power Injection Method test displaying excitation through shaker on the upper wing; on the right, SEA model to predict vibro-acoustic response, and detail showing the air gaps size

The specimen was subjected to a test to apply the Power Injection Method considering excitation only in the three structural elements (the three wings, see Figure 2) installing instrumentation to measure the input power applied through an accelerometer and a force cell at the excitation point and to measure the response of the wings to the input power distributing approximately twenty accelerometers on each panel (see Figure 3). To simulate a non-contact excitation, each wing was excited in three different and randomly distributed points averaging afterwards the resulting energetic states. The test was performed on a frequency range covering the third of octave bands spectrum from 100 Hz to 4000 Hz.

In comparison with the model oriented for acoustic prediction depicted in Figure 17, from the selection of subsystems identified for the specimen studied, a SEA model was developed to be updated through the methods proposed within this work. The SEA model includes the five identified subsystems: three panels and two air layers. Under the scope of this work some considerations were analysed on including the join of the different subsystems. As Figure 2 shows, the three panels are connected through two different elements: a first element, made of six connecting elements, part of the Hold Down System, that link the three panels together and a second element, made of two hinges that link each panel only to the contiguous one. On the SEA model proposed to be updated only the second element is considered, so no direct connection between bottom and upper panel is assumed. A sketch of the SEA model, showing the elements considered, is depicted in Figure 18.



Figure 18. SEA model of the ARA-MK3 solar array in stowed configuration considering the three wings, the two air layers and only connection between contiguous wings through hinges on the lateral side of the wings

Similarly as for the analytical model, two approaches are considered on this work:

- Excitation and measurement are feasible in the three wings that are also all the subsystems considered (full internal and external knowledge), evaluating the effective dissipation matrix.
- While measurement in the three wings is considered, only excitation on the external ones is considered providing only two energetic states of the system (full internal knowledge, partial external knowledge), evaluating the effective dissipation matrix.

The proposed updating methodology is applied to the tested specimen from the output data of the PIM test performed. From the systems response on frequency, two different behaviours are identified and for the sake of clarity the results are presented in two frequency ranges separately. Together with the SEA reduced loss factors predicted by the two approaches stated, the corresponding reduced SEA loss factors of the model to update are shown as reference in grey.

The SEA loss factors predicted through the first approach, considering injection of power input in the three subsystems analysed are shown in Figures 19 and 20.

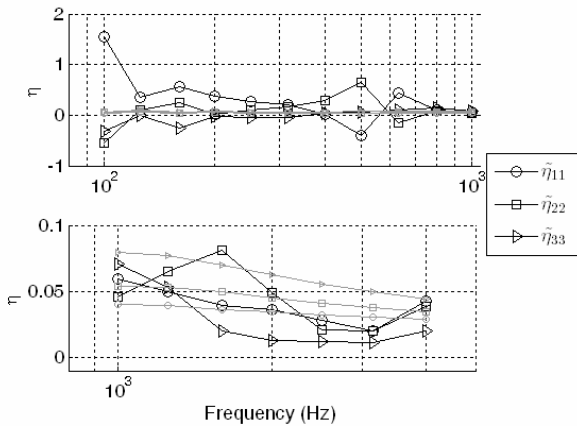


Figure 19. Updated ILF of the reduced model (three wings) considering three power states through excitation on the wings. The SEA loss factors of the model to update are displayed in grey.

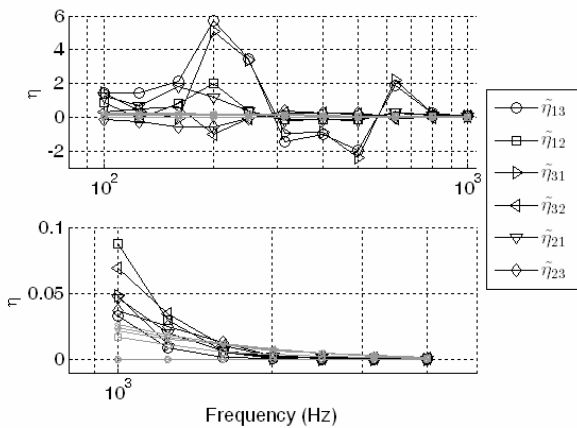


Figure 20. Updated CLF of the reduced model (three wings) considering three power states through excitation on the three wings. The SEA loss factors of the model to update are displayed in grey.

The updated SEA loss factors corresponding to the reduced system allow reproducing more adequately the measured response of the systems. As stated, the proposed model to be updated through the procedures presented does not include a direct connection between the bottom and top wings as is present on the actual specimen. The updated effective loss factors corresponding to the interaction between bottom and upper panels (η_{13} and η_{31}), of the order of the connections included on the model (between contiguous panels) provide in the updated model the actual direct connection.

The SEA loss factors predicted through the second approach, considering injection only on two of the three subsystems considered (the external wings) are shown in Figures 21 and 22.

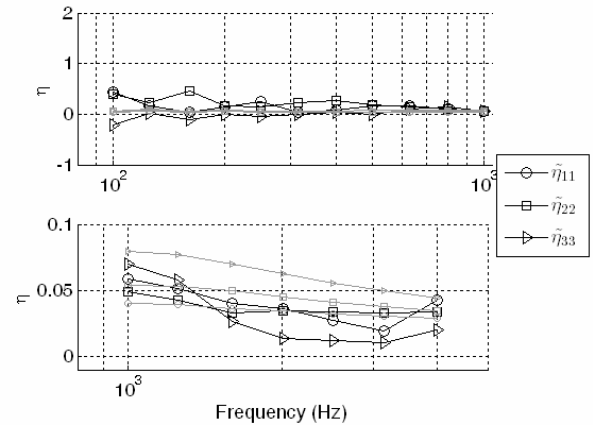


Figure 21. Updated ILF of the reduced model (three wings) considering two power states through excitation on the external wings only. The SEA loss factors of the model to update are displayed in grey.

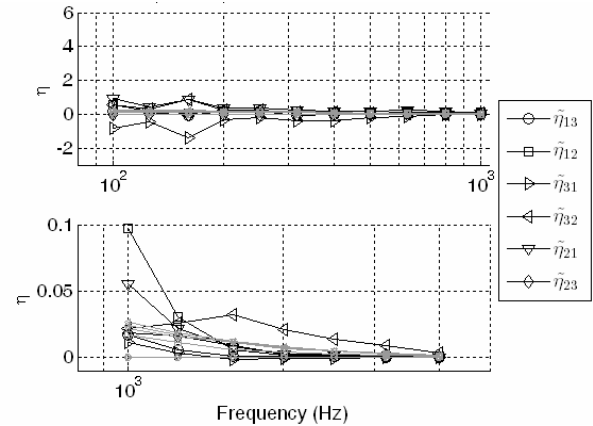


Figure 22. Updated CLF of the reduced model (three wings) considering two power states through excitation on the external wings only. The SEA loss factors of the model to update are displayed in grey.

The same updating trend, including the direct connection between bottom and upper panels, (η_{13} and η_{31}), is found on the results of this approach despite the lower level of knowledge on the response of the system. This restriction on the number of power states considered does have a general influence on the predicted values of the loss factors associated to the non-excited subsystems: both the internal loss factor (η_{22}) as well as the coupling loss factors associated to the transfer of power from the excited subsystems to the non-excited one (η_{12} and η_{32}). In general, a better agreement and a lower need of updating are found on the loss factors associated to the excited subsystems.

CONCLUSIONS

The influence of the selection of subsystems for the evaluation of the SEA loss factors matrix has been presented. In general, the loss factors matrix determined through the application of the Power Injection Method is not the theoretical one corresponding to the whole system but an effective reduced loss matrix. The relationship between the

whole loss matrix and the effective loss matrix has been identified.

The air gap can result to be essential for reproducing and studying the behaviour of stacked structures, as solar panel arrays in folded configuration. The influence both on the magnitude and on the character, of the terms of the loss factor matrix is important. If available measurement does not correspond to all the elements of the system, and only measuring of a reduced set subsystem are available, the identification process does not correspond to the original subsystems. Simulated and experimental results are in agreement with the reduced system results.

The particularities of the effective loss matrix that relates the power applied on the tested subsystems in which measurement is possible have been presented, pointing out that the corresponding loss factors do not have to comply necessarily with the SEA canonical restrictions on their sign.

The particularities of the configurations on present solar arrays in their stowed configurations, and the restrictions that imply for the application of the PIM have been presented. These ones are usually related to the capacity to excite all the subsystems of interest and the degree of knowledge on the response of the system when the response in some sections can not be measured.

Different procedures based on updating techniques have been presented. These procedures have the scope of determining the SEA loss factors through the minimization of a functional that takes into account the energy balance from the input power states tested. From the application of the procedure proposed, connections between elements of the system not considered in the initial model proposed can be identified and included in the updated model.

The proposed procedure also allows obtaining the SEA loss factors matrix of the whole system including the non-excited subsystems through the formulated updating process. Results show that precision of the coupling and internal loss factors in the excited and measured subsystem is adequate. The estimation of couplings and internal factors of the unmeasured subsystems results to be enough adequate for the model development.

The procedures presented here provide a new loss factors matrix to be used on the additional analysis of the specimens and deepens in the behaviour of the system, useful for testing design and correlation tasks.

ACKNOWLEDGEMENTS

This work has been supported by European Space Agency, under the frame of work DS-P-07-239-1 with Dutch Space, and the Spanish Ministry of Science and Innovation under the research programs DPI2005-08276 and PB98-0725.

REFERENCES

1. R.H. Lyon and G. Maidanik, "Power flow between linearly coupled oscillators"; *J. Acoust. Soc. Am.* **34**, 632-639 (1962)
2. R.H. Lyon, *Statistical energy analysis for designers. Part I Basic Theory* (ADIA-006 413 National Technical Information Service, Cambridge Massachusetts, September 1974).
3. F.J. Fahy, "Statistical Energy Analysis. A critical overview" *Philosophical transactions: Physical science and technology.* **346**, 437-447 (1994)
4. D.A. Bies and S. Hamid "In situ determination of loss and coupling loss factors by the power injection method", *J. of Sound and Vibr.* **70**,187-204 (1980).
5. N. Lalor, "Measurement of SEA loss factors on a fully assembled structure". *ISVR TR 150*. August 1987.
6. V. Cotoni and P. Shorter "Modelling the response of stacked solar arrays: Impact Analysis." *Spacecraft and Launch Vehicles Dynamic Environments Workshop 2009*
7. J.J. Wijkker, "Acoustic effects on the dynamic characteristics of light weight structures" *MSC/Nastran European Users' conference.* (1985)
8. J. López-Díez, F. Simón, M. Chimeno and J. J. Wijkker; "Influence of gap thickness on the vibroacoustic response of satellite solar panels". *Inter-Noise Congress 2010*
9. C. Hopkins, "Experimental Statistical Energy Analysis of coupled plates with wave conversion at the junction" *J. of Sound and Vibration* **322**, 155-166 (2009)
10. K. Renji and M. Mahalakshmi, "High frequency vibration energy transfer in a system of three plates connected at discrete points using statistical energy analysis" *J. of Sound and Vibr.* **296**, 539-553 (2006)
11. R. J. Guyan, "Reduction of stiffness and mass matrices", *AIAA J.*, **3(2)**, 380 (1965).
12. B. M. Irons, "Structural Eigenvalue Problem; Elimination of unwanted variables", *AIAA J.*, **3(5)**, 962-962 (1965).
13. M. Baruch, P. García-Fogeda, J. López Díez, J. and V. Marco; "A parametric identification technique for nonlinear dynamic system Spacecraft Structures and Mechanical Testing", ed. CNES/ESA (Spacecraft Structures and Mechanical Testing, Cépaduès-éditions, ISBN 2.85428.364.3; 327-339, 1994)
14. M. Baruch, "Optimization procedure to correct stiffness and flexibility matrices using vibration test". *AIAA J.* **16**, 1208-1210 (1978)